

ELIMINATION OF THE HOOK EFFECT USING MICROFLUIDIC VALVES

BY

NICHOLAS LEMOS

A THESIS SUBMITTED IN PARTIAL FULFILLMENT OF THE

REQUIREMENTS FOR THE DEGREE OF

MASTER OF SCIENCE

IN

MECHANICAL ENGINEERING

UNIVERSITY OF RHODE ISLAND

2018

ProQuest Number: 10982933

All rights reserved

INFORMATION TO ALL USERS

The quality of this reproduction is dependent upon the quality of the copy submitted.

In the unlikely event that the author did not send a complete manuscript and there are missing pages, these will be noted. Also, if material had to be removed, a note will indicate the deletion.



ProQuest 10982933

Published by ProQuest LLC (2018). Copyright of the Dissertation is held by the Author.

All rights reserved.

This work is protected against unauthorized copying under Title 17, United States Code
Microform Edition © ProQuest LLC.

ProQuest LLC.
789 East Eisenhower Parkway
P.O. Box 1346
Ann Arbor, MI 48106 – 1346

MASTER OF SCIENCE THESIS
OF
NICHOLAS LEMOS

APPROVED:

Thesis Committee:

Major Professor Mohammad Faghri
Constantine Anagnostopoulos
Yi Zheng
Stephen Powers
Nasser Zawia
DEAN OF THE GRADUATE SCHOOL

UNIVERSITY OF RHODE ISLAND

2018

ABSTRACT

The Hook Effect is a phenomenon that occurs within microfluidic tests, whereby a reduced signal response is observed as a result of an over-abundance of analyte. This study demonstrates the development of a microfluidic chip device that significantly reduces the impact of the Hook Effect in sandwich assays. This is achieved through the conception, characterization, and implementation of a novel microfluidic valve, The mono-material cantilever valve. This valve uses the capillary behavior of fluid traveling through paper to straighten out a bent beam of paper. The straightened piece of paper contacts a channel on the other end, meaning the fluid on the other side is held in place until the valve is actuated. The new microfluidic chip, dubbed the SuperLoop, uses two cantilever valves to sequentially apply a wash step, followed by the gold-nanoparticle connected antibodies automatically after the user adds sample fluid. This process washes away the excess analyte, reducing the presence of the hook effect in fluidic tests being run at high concentrations. For the purpose of developing and testing this device, commercially available pregnancy tests were tested at high hCG concentrations to isolate the Hook Effect within them. The hook effect was determined to occur with sample fluid hCG concentrations ranging from $1.092 \times 10^6 \text{IU/L}$ to $1.092 \times 10^9 \text{IU/L}$. The active components were then removed from these tests and placed within the SuperLoop device, and this new device was tested at the same concentrations. The results of both tests were then compared, and the SuperLoop's performance was analyzed. The SuperLoop showed a 38.5% reduction in Hook Effect spread.

ACKNOWLEDGMENTS

Without the assistance of many great people, this project would not have been possible. Firstly, I would like to thank Dr. Mohammad Faghri for first bringing me into this project, and supporting me throughout its completion. If he had not asked for volunteers in that fateful Heat and Mass Transfer lecture, I would have missed out on my undergrad research, two summer internships, a TA position, and this Master's project!

I would also like to thank Dr. Constantine Anagnostopoulos, who always had time to chat about chip ideas and helped me to overcome my tendency to respond to any difficulty with a complete redesign of the device!

I have to thank Manuel "Manny" Muller, who provided me with my initial training in microfluidic device manufacture when I started as an undergrad researcher, and continued to provide ideas and guidance all the way up to this thesis.

I owe a great deal of thanks to Santiago Sanchez, who provided me with CorellDRAW and microfluidic device design training. The work we did together on housings also served as my introduction to 3D printing, which has come in handy many times in and outside of this project.

I want to thank Yaser Kashcooli for providing a great deal of assistance with the early isolation of the Hook Effect and valve experiments. In addition to this, He also served as a great source of quick answers to chemistry questions.

I must thank Winfield "Wayne" Smith, who was an inexhaustible source of ideas and potential solutions to problems. His work with bi-material cantilever valves also served as the inspiration for the mono-material valve used in the final version of this device.

I also have to thank the other members of the lab on a chip crew, whose

company prevented me from becoming a total hermit during my research. Ramata "Rama" Sidibe was my first partner in this project. In addition to making the summer internship much more fun, working with Her gave me the confidence to instruct new students in the fabrication of microfluidic devices. Brenno Ribeiro's endless positivity and helpfulness served to motivate me when I was feeling stressed. Amer Abdul Razeq Charbaji also provided me with many good ideas and conversations throughout our time together.

Lastly, and probably most importantly, I must thank my family. Without their constant support I never would have been able to start this project, let alone finish it. Whether they were providing me with rides, ideas, emotional support, ego deflation services, or just a good laugh, they were instrumental in the completion of this project. They probably deserve degrees of their own just for putting up with me this long. But they cannot have this one, because it is mine.

TABLE OF CONTENTS

ABSTRACT	ii
ACKNOWLEDGMENTS	iii
TABLE OF CONTENTS	v
LIST OF FIGURES	viii
LIST OF TABLES	x
1 Introduction	1
1.1 Background	1
1.2 Mechanics of Immunoassays	1
1.3 The Hook Effect	2
1.4 Paper Based Microfluidic Devices	4
1.5 Objective and motivation	4
2 Review of Literature	6
2.1 The Hook Effect	6
2.1.1 The Hook Effect in Pregnancy Tests	6
2.1.2 The Hook Effect in Other Medical Tests	7
2.2 Microfluidic valves	8
2.2.1 Externally Triggered Valves	8
2.2.2 Automatic Valves	8
2.3 Mechanics of Fluid Flow Through Paper	9
2.3.1 Washburn Equation	9
2.3.2 Darcy's Law	10

	Page
2.3.3	Capillary Action 11
2.3.4	Practical Experiments 11
3	Methodology 13
3.1	Isolation of the Hook Effect 13
3.1.1	Mixing hCG Solution 13
3.1.2	Running and Scanning Pregnancy Tests 14
3.1.3	Processing chip scans using ImageJ 15
3.2	Chip Manufacture 15
3.2.1	Materials 15
3.2.2	Equipment 16
3.2.3	Assembly 18
3.3	Chip Design 19
3.3.1	Principles of design 19
3.3.2	SuperLoop chip concept 20
3.4	Valve Design 21
3.4.1	Allyltrichlorosilane Valve 22
3.4.2	Wax Based Valve 25
3.4.3	Cantilever Valve 26
3.5	Valve Characterization 27
3.5.1	Bi-material Valve Testing 28
3.5.2	Mono-material Valve Testing 29
3.6	SuperLoop Design 31
3.7	Testing New Device 32

	Page
3.7.1	Fluidic Testing 32
3.7.2	Hook Effect Mitigation Testing 33
3.7.3	Running and Scanning New Device 33
3.7.4	Processing results using ImageJ 34
4	Findings 35
4.1	Isolation of the Hook Effect 35
4.2	Characterization of the Cantilever Valve 35
4.2.1	Bi-Material Valve Characterization 35
4.2.2	Mono-Material Valve Characterization 36
4.3	SuperLoop Hook Effect Mitigation Results 38
5	Conclusion 42
5.1	Future Work 42
5.1.1	Hook Effect Mitigation Device Refinements 42
5.1.2	Applying SuperLoop device to other Sandwich ELISA Tests 44
5.1.3	Future Applications of Cantilever Valve 44
5.1.4	Continuation of Abandoned Valve concepts 44
	LIST OF REFERENCES 46
	BIBLIOGRAPHY 48

LIST OF FIGURES

Figure		Page
1	Cross section of a common Immunoassay [1]	2
2	Graph Showing the Hook Effect [2]	3
3	Ordinary Sandwich Assay Performance (A) vs Hook Effect (B) [3]	4
4	Results of DcR2 Hook Effect Study [4]	7
5	Washburn Equation [5]	9
6	Simplified Washburn Equation [6]	10
7	Darcy’s Law [6]	10
8	Simplified Darcy’s Law [6]	10
9	Laser cut blotting paper parts used in the final device	17
10	3d model of original single valve chip design	18
11	SuperLoop Print	19
12	SuperLoop Cut	20
13	SuperLoop Device Diagram	21
14	Outer Vapor Chamber	23
15	Inner Vapor Chamber	24
16	Wax Valve Prototype	25
17	3D printed valve test base	28
18	Cantilever Valve Bending Jig	29
19	Mono-material Length Characterization Test	29
20	SuperLoop Chip Part	31
21	Disassembled Pregnancy Test	32

Figure		Page
22	Fluidic SuperLoop Test	33
23	Signal Response Over hCG Concentration in Common Preg- nancy Tests	35
24	Results of Mono-Material Minimum Fluid Test	38
25	25 by 25 Scan of SuperLoop vs Unmodified Device	39
26	Full Area Scan of superLoop vs Unmodified Device	39
27	25 by 25 Scan of SuperLoop vs Unmodified Device Normalized .	40
28	Full Area Scan of superLoop vs Unmodified Device Normalized	40

LIST OF TABLES

Table		Page
1	Bi-material Cantilever Performance	36
2	Mono-material Cantilever Performance With Various Lengths .	36
3	Mono-material Cantilever Performance With Various Widths . .	37
4	Mono-material Cantilever Performance With Various Fluid Vol- umes	38
5	Performance of SuperLoop vs ordinary test at hook effect con- centrations	41

CHAPTER 1

Introduction

1.1 Background

Immunoassays are an increasingly popular method of detecting the presence of a particular substance in the modern world. In the form of point of care (POC) tests, they are used for a wide variety of medical applications, including tests for pregnancy, steroid use, and syphilis. [7] Their portability, fast turn around time, and cost effectiveness make them an attractive option for medical professionals and consumers all over the world. According to MarketsandMarkets, the total market value of point of care diagnostics is projected to grow to \$38.13 billion by 2022.[8] The popularity of this type of test is most evident in the prevalence of low cost, high quality pregnancy tests. Despite their ubiquity, these tests still have limitations that can cause real world problems. Chief among these is the so called hook effect, also sometimes referred to as the Prozone effect.

1.2 Mechanics of Immunoassays

Immunoassays are medical tests that use antibodies to detect a particular target molecule. This target molecule is known as the analyte. [1] There are many different types of immunoassay, but this study is concerned primarily with the sandwich assay POC test. This test gets its name from the "sandwich" that forms between the analyte and the two antibodies in the test during normal operation. The test consists of a porous strip with a quantity of antibody affixed to it, commonly referred to as the test line. A piece of hydrophilic material holds a second, free floating antibody connected to a visible particle, typically a gold nanoparticle. This part is commonly referred to as a conjugate pad, and is typically made of glass fiber. The conjugate pad is fixed to the strip in front of the test line.

When a sample is added to the chip the target molecule, or analyte, binds to the free-floating antibody. The antibody-analyte pair then flows into the test line and binds to the fixed antibody. This retains the visible particle within the porous structure of the test line. A great quantity of these structures allows for a visible indication on the test line of the strip [1].

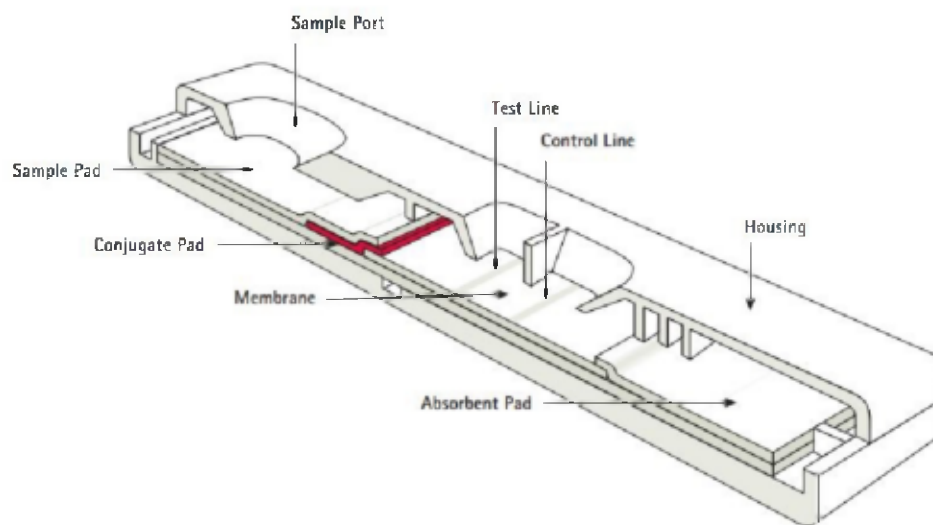


Figure 1. Cross section of a common Immunoassay [1]

1.3 The Hook Effect

The Hook effect, also known as the Prozone effect, is a problem inherent in immunoassay tests. The effect manifests as a reduction in signal response that appears when there is an overabundance of the target molecule in the sample being tested. The name comes from the hook that appears on a graph of signal response over concentration of analyte, as shown in Fig. 2

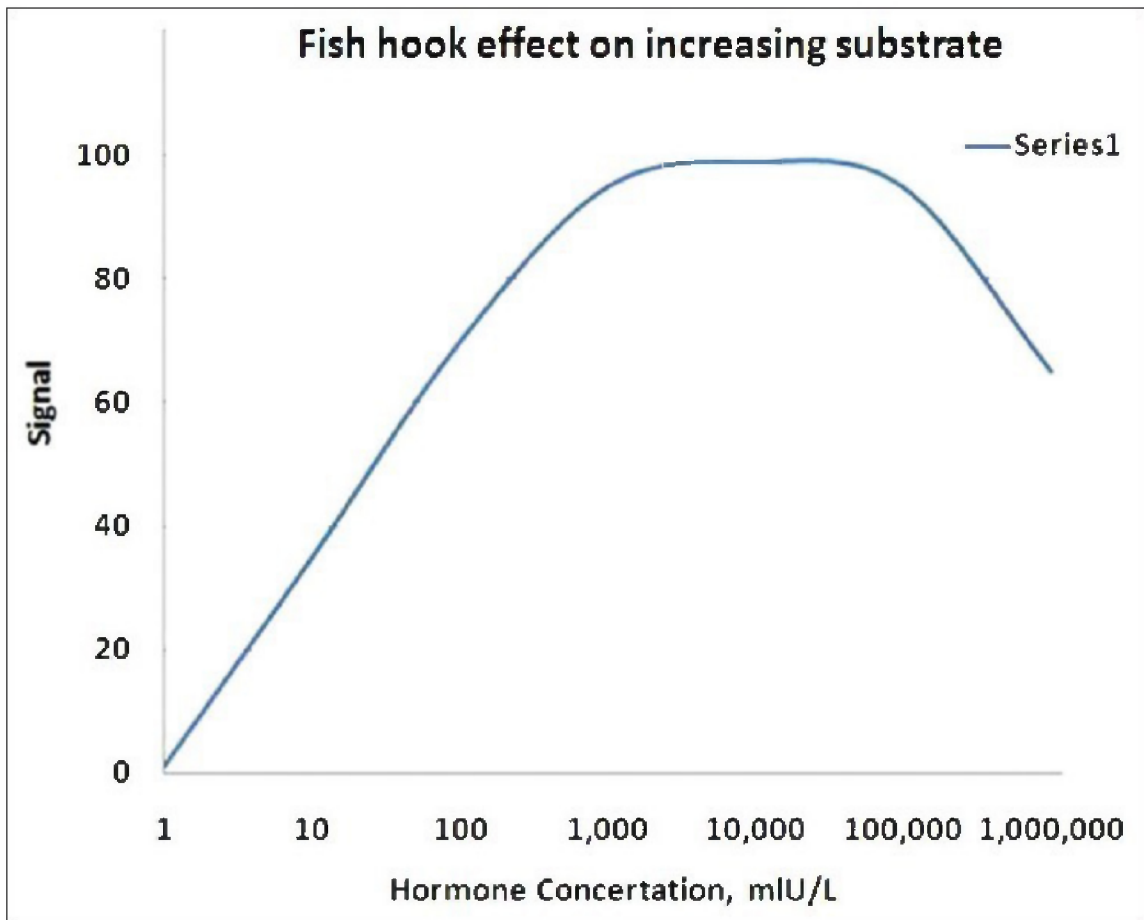


Figure 2. Graph Showing the Hook Effect [2]

This effect is caused by the disruption in the structure of the sandwich assay that occurs in the presence of too much analyte. If the quantity of analyte is great enough, there can still be unbonded analyte molecules after all the free-floating antibodies have bonded. When the sample fluid reaches the test line, some or all of the fixed antibodies will be occupied by analyte molecules that have not bonded to the free-floating analyte. Thus the sandwich is not completely formed, and fewer visible particles are facing up on the test line, as seen in the B section of Fig. 3. This accounts for the drop in signal response that occurs at higher analyte concentrations. [9] This effect is responsible for false negatives in pregnancy tests as well as other types of immunoassays, like syphilis tests.[7]

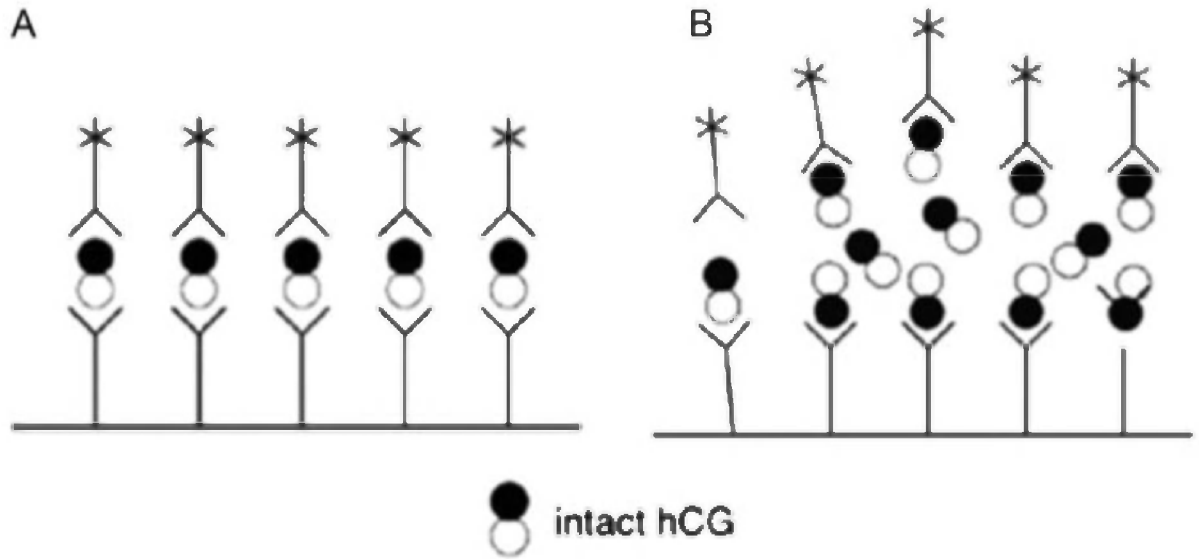


Figure 3. Ordinary Sandwich Assay Performance (A) vs Hook Effect (B) [3]

1.4 Paper Based Microfluidic Devices

Paper Based Microfluidic Devices (PBMD's) allow simple fluidic operations to be automated within a single chip. These devices typically consist of paper channels and Paper Based Microfluidic Valves(PBMV's). The arrangement of these channels and valves allows for control over the motion of fluids within the device. The control of fluids allows for multi step processes that normally require a lab to be performed within a single device. Both Wilke Follischer and Manuel Muller developed PBMD's in the URI microfluidics laboratory, and their research helped to pave the way for this study. [10, 6]

1.5 Objective and motivation

The purpose of this study is the elimination or mitigation of the hook effect in POC microfluidic tests. In order to accomplish this the hook effect must first be isolated in a commercially available sandwich ELISA test that is vulnerable to the Hook Effect. Pregnancy tests are an excellent example for this study, because although the tests themselves are fairly reliable, the hCG levels in pregnant women

can vary wildly over the course of the pregnancy.[2] Therefore a universal method of mitigating this effect will be extremely useful if this technology is to continue to grow.

After the hook effect has been isolated in a pregnancy test, a multi fluid system in which the addition of the sample fluid automatically triggers a wash step will be developed. This will be achieved by the application of the PBMV technology being developed by Lab on a Chip LLC in URI's microfluidics laboratory. The development of this new multi fluid system will also spur the development of a novel valve concept that will open up new chip design possibilities. The completion of this research will not only provide a method for mitigating the Hook Effect, but will also help to further advance the development of PBMD technology.

CHAPTER 2

Review of Literature

2.1 The Hook Effect

The hook effect presents significant problems to the medical industry, and thus many studies have been performed on its mechanics and impact.

2.1.1 The Hook Effect in Pregnancy Tests

One excellent article, published in the Journal of Emergency Medicine, investigated recorded cases of false negative results from POC pregnancy tests caused by the hook effect. [3] The article explains how exceedingly rare these cases are, proposing a 0.19% false negative rate based on the data being analyzed. It then goes in detail on the individual cases being studied. In these cases, the more reliable, quantitative blood serum test was run after the urine test came back negative. Serum hCG tests ranged in concentration from $2.54 \cdot 10^4$ IU/L to $2.68 \cdot 10^8$ IU/L. The article then goes on to explain the difficulties with POC pregnancy tests, noting the fact that hCG concentrations in the urine of pregnant women vary wildly with stage of pregnancy, hydration and other factors. Even if this problem is rare, its presence in such a well developed test still indicates a promising area for research and development.

Another article, published in the journal Gynecologic Oncology Reports, describes the phenomenon of molar pregnancy and its relation to the Hook Effect. [9] According to the article, about half of molar pregnancies result in serum hCG levels greater than 100,000 IU/L, and the Hook Effect can begin to occur with serum levels greater than 500,000 IU/L. The article then goes on to describe a particular case of molar pregnancy where the Hook Effect caused a false negative on initial tests, only to reveal an hCG serum level greater than 900,000 IU/L after

proper dilution. The article then goes on to discuss the mechanics of the hook effect as were discussed in section 1.

2.1.2 The Hook Effect in Other Medical Tests

The hook effect has been observed in ELISA tests for DcR2. In one study published in the Journal of Clinical Biochemistry, the Hook Effect was studied in cases of patients with kidney disease being tested for DcR2 using POC urinary tests. [4] The article explains that DcR2 is a biomarker that can be used to detect tubulointerstitial injuries (TII). This study showed that the test indications could be significantly improved in patents with severe TII through dilution of the urine prior to testing. Fig.4 shows the results of the study, illustrating how the tests results could be improved through 4-fold dilution of urine prior to testing for all patients with TII, with the greatest gains being observed in the most severe cases. An automated system capable of performing this dilution would greatly improve the effectiveness of a test like this as well.

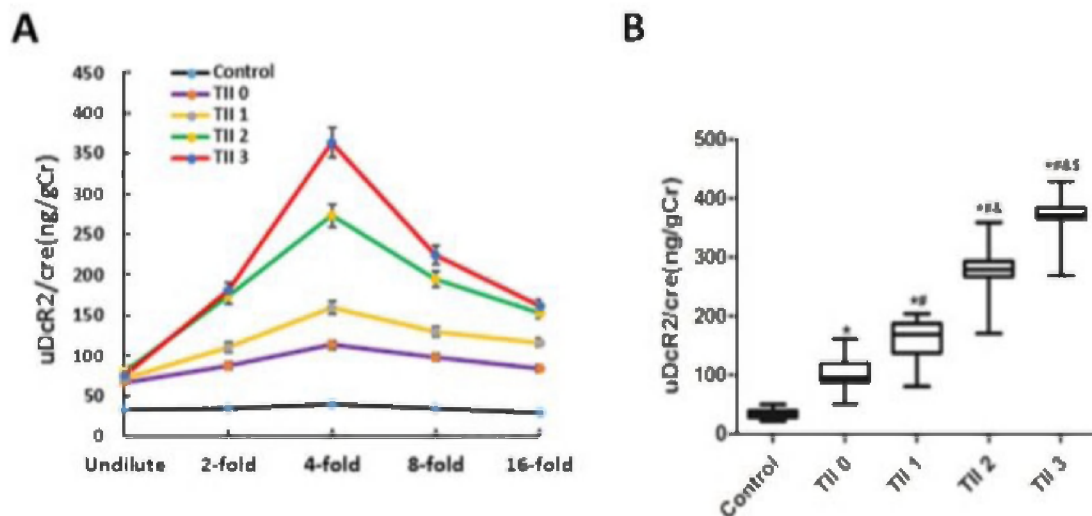


Figure 4. Results of DcR2 Hook Effect Study [4]

A similar individual case of the Hook Effect was documented in the Indian

Journal of Sexually Transmitted Diseases.[7] In this case, a woman tested negative for secondary syphilis despite showing symptoms. After running the test again with a 1:512 dilution sample fluid, the test came back positive. In this case the symptoms were obvious, so the doctors knew to look more carefully, but in situations where illness is not obvious, the hook effect could result in people not receiving treatment when it is needed.

2.2 Microfluidic valves

There have been many advancements in the development of microfluidic valves in the last 10 years, many of which were made in the URI microfluidics laboratory.

2.2.1 Externally Triggered Valves

Many microfluidic valves that must be triggered through some external means have been designed over the years. Though not ideal for POC devices, studying them can nonetheless help build an understanding of valve design and serve as potential inspiration for new ideas. A paper published in Analytical chemistry put forward a valve design that is manually actuated by the user. [11] This valve consisted of a fluidically conductive channel that could manually be slid into position to connect to points on a fluidic circuit. This allowed the user to connect and disconnect points on the circuit at will. While this concept was not used directly it did help inspire the mono-material cantilever valve discussed later.

2.2.2 Automatic Valves

Many of the valves used in the URI microfluidics laboratory have been automatically actuated. Wilke's thesis was based around using these devices for automation of fluid control within a microfluidic device.[6] The valve used in Wilke's project consisted of a disk treated with a hydrophobic solution placed on top of a disk treated with surfactant. The hydrophobic disk held back reagent applied to

hydrophilic paper above it. When the sample fluid approached the valve from below it would mix with the surfactant, and the surfactant solution would penetrate the hydrophobic disk. These valves, and a chip composed of paper treated with wax patterns to create delay channels, fluids could be sequentially loaded into the chip automatically.

2.3 Mechanics of Fluid Flow Through Paper

There are several methods which are useful for analyzing the flow of liquid through porous media. Each of these methods will be explored in detail and related to the larger project.

2.3.1 Washburn Equation

The Washburn equation is used to describe the penetration of fluid into a dry material.

$$x = \sqrt{\frac{\gamma \cos\theta}{\mu} \frac{r_c t}{2}}$$

Figure 5. Washburn Equation [5]

In this form of the equation γ is the surface tension, μ is the viscosity, θ is the contact angle, r_c is the average pore radius, and t is time. x represents the distance into the dry porous media the fluid will flow. This equation can be simplified by assuming the angle of contact will be 0, as the fluid is flowing straight through the paper. By applying this, changing x to a more descriptive length L , and replacing the r_c term with the pore diameter $D/2$ the version of the equation used by Wilke in his thesis can be derived.

$$L = \sqrt{\frac{\gamma Dt}{4\mu}}$$

Figure 6. Simplified Washburn Equation [6]

This equation describes the behavior of the material at the head of the fluid flow, but another equation is required to model the flow of the fluid within the already wet portions of the channel.

2.3.2 Darcy's Law

Darcy's law allows for the flow of fluid within wetted portions of the channel to be predicted.

$$Q = -\frac{\kappa WH}{\mu L} \Delta P$$

Figure 7. Darcy's Law [6]

In this formula Q represents the volumetric flow rate, k is the permeability of the medium, W is the width of the channel, H is the height of the channel, μ is the viscosity again, L is the length of the channel, and ΔP is the pressure differential across the channel. If the cross sectional area of the channel is constant, then the formula can be reduced to:

$$q = -\frac{\kappa}{\mu L} \Delta P$$

Figure 8. Simplified Darcy's Law [6]

In this simplified form q represents the the flow rate in the channel. This equation is relevant to the research at hand, as the transport of nanoparticles within the chip will be affected by the flow rate.

2.3.3 Capillary Action

Capillary action describes the balance between attractive and repulsive forces that cause fluid to move through porous media.[12] Both of these forces occur on a molecular level. Cohesion forces occur between particles of the same type of matter, while particles in the vicinity of a different type of mater are subject to Adhesion forces. In the context of this study, adhesion forces occur between the fibers of the paper and the fluid running through the tests, while cohesion forces occur between individual particles of the fluid. Capillary action occurs in any porous media exposed to fluid, but the simplest case, and thus the best model for this phenomenon, is a glass tube with a internal diameter equivalent to the external diameter of a human hair. A tube of this type placed partially in water will have water within it rise above the waterline. This same force is what compels fluid to flow through porous media like paper.

2.3.4 Practical Experiments

In addition to these mathematical models, practical experiments have also been performed on the flow of fluid through porous media. One such study was performed on Whatman chromatography paper by researchers at the University of Ontario Institute of Technology [5]. This group analyzed the effects of geometry, flow direction. temperature, and humidity on the flow rate of water through Whatman 1 CHR and Whatman 17 CHR paper. The study concluded that ambient humidity and strip length had no significant effect on fluid flow rate. The width, however, was determined to have a significant effect on only one of the two

varieties of paper the group tested. The 0.18mm thick CHR 1 material showed faster saturation times with increasing strip width, while the 0.70mm thick CHR 17 paper showed no significant variation under the same conditions. The orientation of the flow within the paper was determined to have a significant effect on the flow rate within the paper as well. The group observed that the fibers within the paper tend to line up with the direction the paper was rolled when it was being manufactured. Their tests confirmed the hypothesis that fluid would travel faster in the direction of manufacture than it did in the perpendicular direction. These practical observations must be taken into account when the new devices are being developed in order to ensure that maximum performance is obtained from all porous media used.

CHAPTER 3

Methodology

This chapter outlines the methods and materials used to design, fabricate and test the hook effect mitigation devices. Several designs were evaluated and rejected before the final version of the device was selected for comprehensive evaluation. Here each step in the iterative design process that lead to the final device is explained.

3.1 Isolation of the Hook Effect

In order to ensure the new devices mitigate the hook effect, the concentrations in which the hook effect occurs must be determined in a commercially available device. Due to their low cost and availability, common pregnancy tests were selected. A large quantity of Clinical Guard urine pregnancy tests were purchased for use in experiments. In order to run these tests, hCG hormone and an appropriate buffer were both purchased as well.

3.1.1 Mixing hCG Solution

The hCG solution was mixed and stored in the following manner:

1. apply all relevant safety equipment, including goggles, a breathing mask, and gloves
2. Lay out hCG vial, hCG Buffer fluid, 50 1000 μ l vials, 100 μ l pipette, 1000 μ l pipette, vortex mixer, and a biohazard disposal bag under a fume hood
3. set 1000 μ l pipette to dispense 1000 μ l
4. open the hCG vial, and add 1000 μ l of buffer fluid to it using the 1000 μ l pipette

5. replace top to hCG vial, and mix for 1 minute continuously using vortex mixer
6. set 100 μl pipette to dispense 20 μl
7. Remove top from the hCG vial, and immediately place it in the biohazard disposal bag
8. using 100 μl pipette, remove 20 μl from hCG vial and deposit it into a 1000 μl vial
9. Seal the 1000 μl vial
10. Repeat steps 8 and 9 until all 50 1000 μl vials are filled
11. Store the newly filled vials in a freezer immediately
12. Place remaining buffer solution into a refrigerator for later use
13. place hCG vial, pipette tips, breathing mask, and gloves into the biohazard disposal bag

This process produced 50 vials of $1.092 \times 10^9 \text{ IU/L}$ hCG solution. When needed, the vials could be retrieved from the freezer, diluted to the appropriate concentration, and used for tests.

3.1.2 Running and Scanning Pregnancy Tests

Each of the strips was dipped down to the suggested line for 5 seconds in the appropriate concentration of hCG solution, then removed and placed flat onto a sheet of aluminum foil. After waiting the manufacturer suggested 5 minutes, each set of strips was placed face down on the scanner. The scanner was set to the maximum resolution 1200 DPI, and the resulting jpeg images were processed using image J software.

3.1.3 Processing chip scans using ImageJ

Each of the obtained scan images was opened in ImageJ. The Invert command was then used to invert the image. A rectangle was then drawn over the line to be measured, with care taken to ensure that the rectangle covered as much of the line as possible without extending off it. The measure command was then used to obtain a numerical value for the presence of color within the drawn rectangle. When the area of the rectangle is completely black, the number returned by ImageJ is zero. The invert command turned the white of the test line into nearly pure black, allowing the color intensity of the test and control lines to stand out. In order to account for the imperfect background in each scan, a value was taken for it by analyzing a 50 by 50 square of the chip backing away from the test and control lines. This value was subtracted from the final value of the control and test lines to obtain adjusted signal values for each. These adjusted signal values were then used to create the graphs displayed in section 4.

3.2 Chip Manufacture

While the devices being manufactured were constantly changing as the project progressed, some manufacturing materials, equipment, and methods remained consistent throughout.

3.2.1 Materials

The fluidic chips were created on sheets of Whatman 41 filter paper. This filter paper is the standard material used by the URI microfluidics lab, as was used by Wilke and the other students who worked on PBMD in the past. It was selected for its relative low cost and high flow rate. [6] Areas of the paper were made hydrophobic using black Xerox Genuine Solid Ink wax.

The waste pads of the PBMD were created out of Millipore blotting paper.

The blotting paper's ability to absorb a large volume of fluid quickly allowed flow to be maintained within the chip. In addition to fluid absorption, the blotting paper also served to provide structural support for the chips that were designed without housings.

The layers of the chip were affixed to each other using FLEXmount select DF071736 double sided tape (DST). This material was chosen for its low cost, low thickness of 0.5 mil (12.7 micrometers), and strong adhesion. In order to facilitate cutting of the material without risking damaging the adhesive, the DST was applied to Reynolds Wrap brand parchment paper. The waxy surface allowed the tape to be easily peeled off after it had been cut.

3.2.2 Equipment

The wax was precisely applied to the filter paper using a Xerox ColorCube 8570 solid ink printer. The wax pattern was created using CorelDRAW 2D design software. The areas to be wax were colored pure black, while all other areas were left blank. The filter paper had to be fed into the manual feed tray one at a time to prevent the pages from sticking. In the printer driver, a default preset file was created to allow the proper settings to be quickly applied. This preset specified the Whatman filter paper size, the manual feed tray, and the maximum picture quality (High Quality) setting. The high quality setting was critical as it ensured that the printer applied the maximum amount of wax to the surface of the paper.

The filter paper, blotting paper, and double sided tape were all cut out using an Epilog Mini 24 laser cutter. For each pattern to be cut, a CorelDRAW file was created. The cuts were represented as vectors of various colors. The Epilog driver allowed the power, speed, and cutting order of the lines to be specified by color. Presets were created in the driver for each material to be cut, with the laser power and speed configured to cut all the way through the material without igniting it.

In addition to the cut presets, a filter paper alignment preset was also created. This preset set the laser power to 0 for every color but pink. The pink lines were set to a power level of 8. This was enough to mark the paper without burning all the way through it. This way the cut could be run on the alignment preset first, and the position of the burned paper could be compared to the pink lines. The ruler printed on each alignment could then be used to shift the image in the driver accordingly to ensure perfect alignment. This is discussed further in the chip design section.



Figure 9. Laser cut blotting paper parts used in the final device

A laboratory pressure oven was used to melt the wax into the paper. This step was critical, as the printer merely applies a dot matrix of wax on to the surface of the paper, so the wax must be melted into the paper fibers to form a truly water-tight seal. The pressure functions of the oven were not used, as consistent temperature was all that was required to ensure proper melting. The oven was set to 140°C and allowed to fully warm up before use. Each wax printed part was placed in the oven for 40 seconds before being removed and allowed to cool.

3.2.3 Assembly

The assembly process also remained mostly consistent for all of the devices produced. A layer of blotting paper was used as a base for all of these chips. Layers of double sided tape and layers of wax treated filter paper were then alternated to build each chip. Fig. 10 shows the structure of an early single valve chip that was assembled using this method.

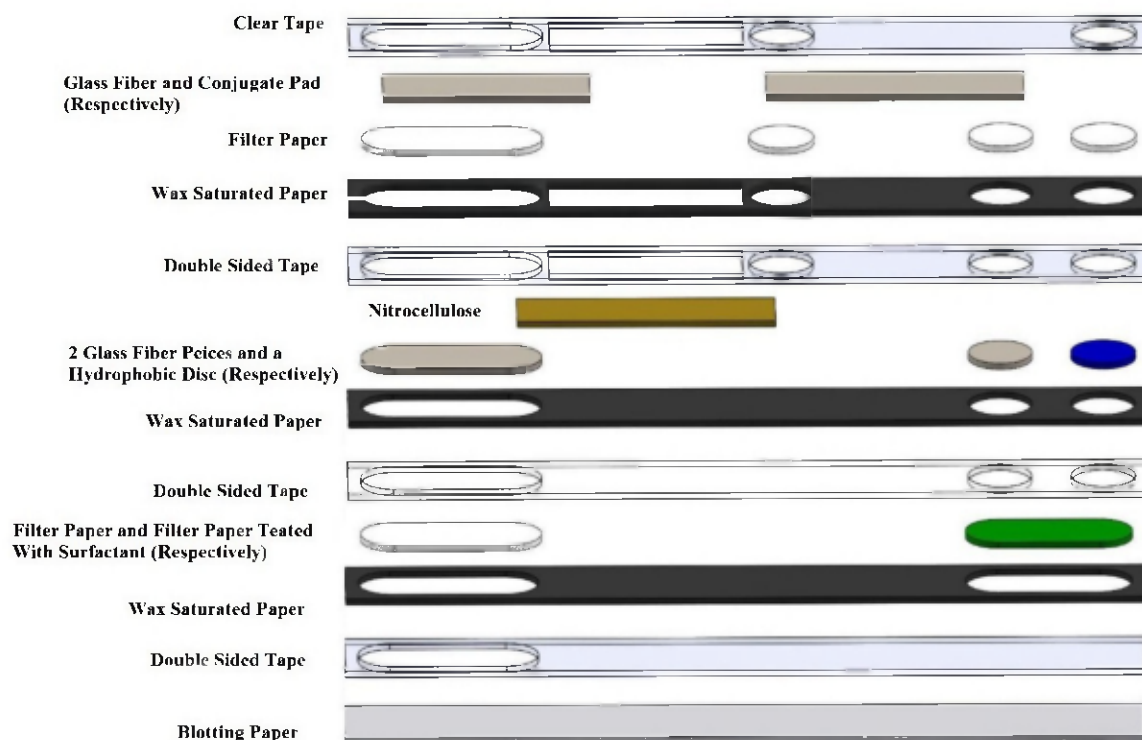


Figure 10. 3d model of original single valve chip design

All subsequent chips were assembled in the same manner, with the only major differences being the preparation of the valves within them. This process is discussed in detail in section 3.4.

3.3 Chip Design

3.3.1 Principles of design

All design work for chip components was performed in CorelDRAW 2d sketching software. The lines for the laser cutter were created as vectors of various colors to allow the order of cuts to be selected. Wax areas were colored in with pure black. An alignment grid was placed on both cut and print files to ensure that the part edges would line up as can be seen in Figs. 11 and 12.

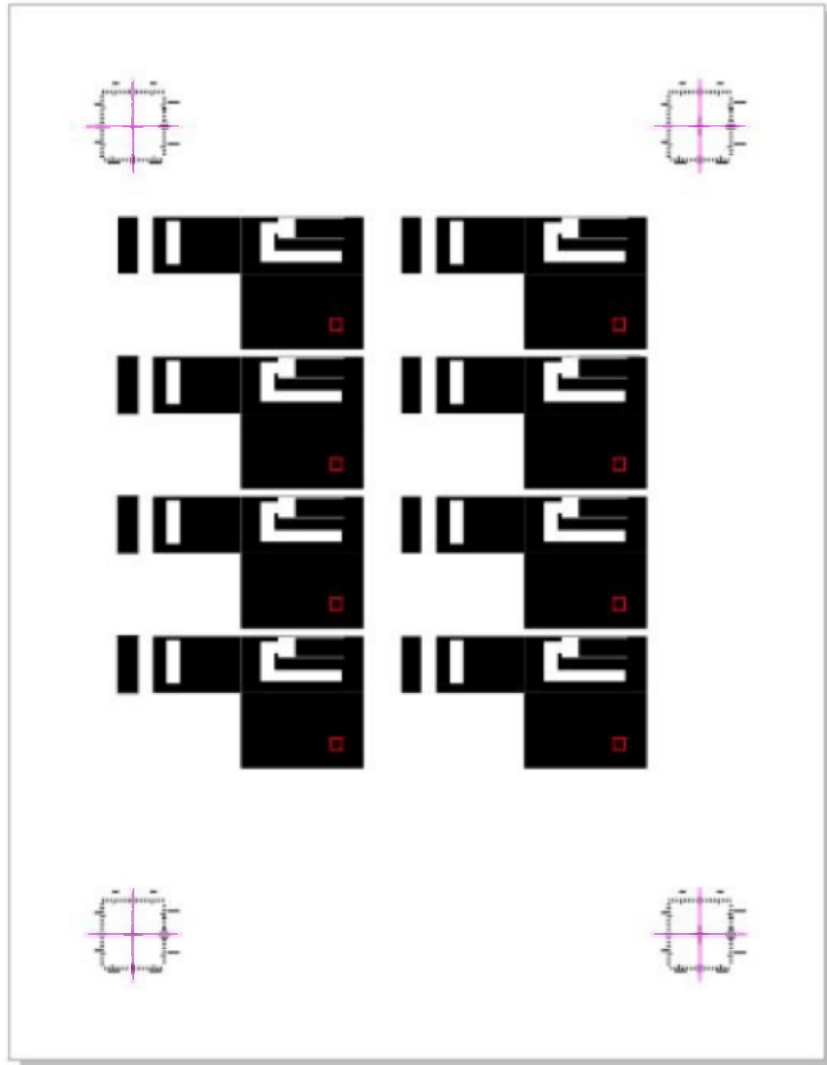


Figure 11. SuperLoop Print

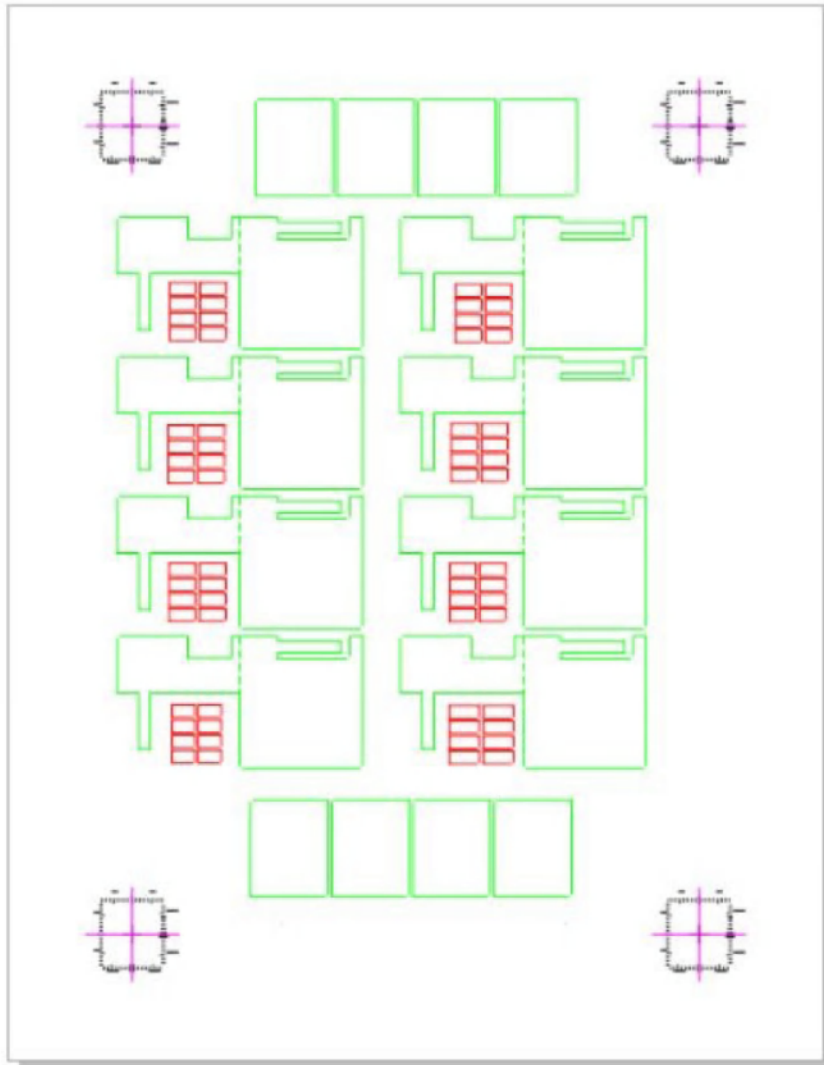


Figure 12. SuperLoop Cut

3.3.2 SuperLoop chip concept

The SuperLoop design used two fluid reservoirs to mitigate the Hook Effect. The initial fluid reservoir was configured to open immediately after the sample fluid was added. This was referred to as the wash fluid. The second reservoir was configured to trigger after the wash fluid. The valve making this connection was set up to connect the reservoir to the test line through the conjugate pad. The fluid contained in this reservoir was referred to as the drive fluid. This system kept the conjugate pad isolated from the rest of the chip until the wash fluid had a chance

to push most of the analyte into the conjugate pad. This way the full sandwich could form at any concentration. The details of the structure and function of the valves are further discussed in section 3.4.3.2.

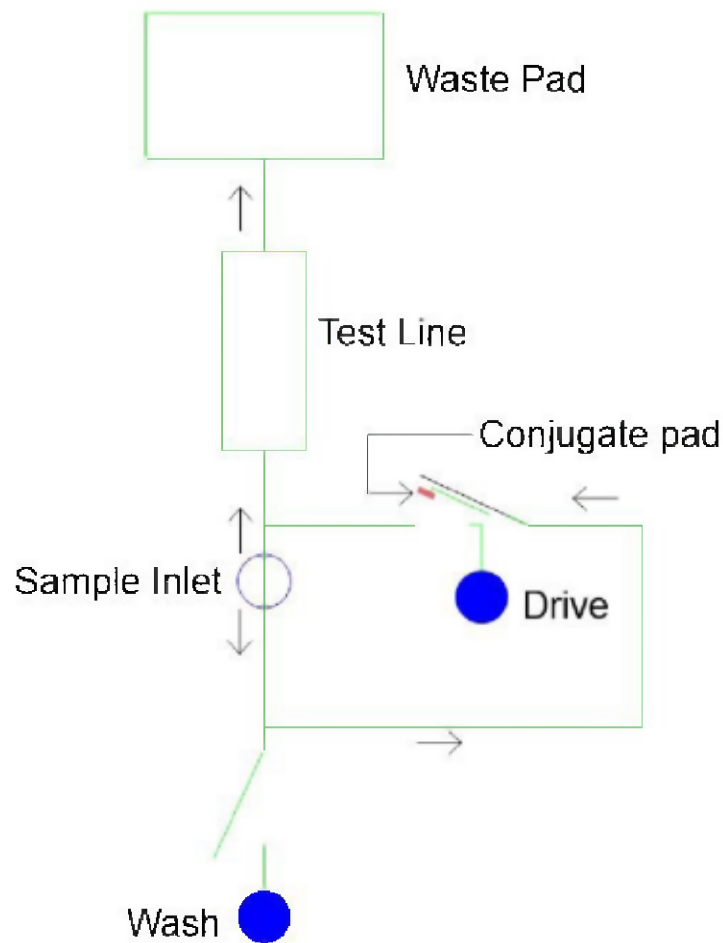


Figure 13. SuperLoop Device Diagram

3.4 Valve Design

Several different valve designs were used in the development of this device. Each of these valves had their own manufacture methods, flaws, and advantages.

3.4.1 Allyltrichlorosilane Valve

As previously discussed, the valves used by Lab on a Chip were based on paper treated with the hydrophobic agent Allyltrichlorosilane (ATCS). Two different methods were used to apply the chemical for this purpose.

3.4.1.1 Pipette Application

The original valve design created by Wilke called for the application of ATCS using a standard step pipette. This allowed for precise application of the fluid. The procedure for the manufacture of this valve was as conducted as follows:

1. Mix solution of ATCS and Perfluoro-compound FC-72 (1 to 8%) by volume
2. Lay out all devices to be treated on aluminum foil
3. Carefully apply 2 to 3 μl of solution
4. Allow to dry overnight before using

While some success was observed in early prototype devices, the valves soon started consistently leaking. After a great deal of tinkering, research, and discussion with colleagues it was determined that the valves were being damaged by humidity. The greatest evidence of this was the sudden decline in performance coinciding with the move of the microfluidics lab from the Kirk building to the Pastore building. In the Kirk building, the lab had an air conditioner and dehumidifier running constantly to ensure the humidity stayed low. In the Pastore building no air conditioners were available, and some of the windows were cracked. Leaving the valve parts out to dry in the open air was compromising their integrity. After this discovery, a desiccant chamber was set up to allow device components to be stored in a low humidity environment. Even with this step, the valves never provided enough reliability to justify a large scale test. Around this time another

student working in the lab was developing his own treatment method in order to increase the reliability of the valves.

3.4.1.2 Vapor Chamber Application

In order to address the shortcomings present in the pipette application method, a new application method was purposed by Winfield "Wayne" Smith. Wayne had the idea to take advantage of ATCL's rapid evaporation when placed in open air in order to treat the devices more effectively.

This new method entailed placing the paper parts to be treated on the floor of a custom made vapor chamber. The vapor chamber consisted of two inexpensive storage bins of the volumes 4.92 liters and 14 liters. The smaller bin had 8 evenly spaced holes in the top in a two by four grid arrangement. Each hole was covered by a 30 mm by 30 mm square of filter paper taped to the bottom of the lid. The larger box was used as a containment unit for the smaller box to protect it during the treatment process. The outer and inner chambers can be seen in Figs. 14 and 15 respectively. The floor of the inner bin was lined with a piece of aluminum foil which had a slight texture applied to it to ensure that vapor could flow under the parts being treated.



Figure 14. Outer Vapor Chamber



Figure 15. Inner Vapor Chamber

The procedure for this treatment method was as follows:

1. Place textured aluminum foil on the floor of the inner vapor chamber bin
2. Evenly distribute all devices to be treated on the aluminum foil
3. place lid on inner vapor chamber
4. Carefully apply 2 to 3 μl of ATCS to each of the paper squares
5. place lid on outer container
6. Leave undisturbed for 12 hours in order to allow parts to absorb the ATCL vapor

The theory was that the enclosed volume of air would protect the devices while they were soaking in ATCL vapor. When the treatment was completed the devices were immediately transferred to the desiccant box to protect them from damage. The small scale experiments performed with these valves never produced consistent enough results to justify a large scale production, so alternative valve concepts were sought.

3.4.2 Wax Based Valve

In order to mitigate the problems with the ATCS valve, a new hydrophobic agent was needed. The chosen agent was the wax that was already being applied to the filter paper in order to create channels. The surfactant laden fluid had already been observed to be able to penetrate into the wax slightly, so this seemed like a logical choice. The hydrophobic disks used in this valve were made using the same method as the chips themselves, with the wax being printed onto and melted into them in much the same manner. The only difference was the wax printer settings. In order to ensure that the valve would be a weak point, the wax was printed onto the hydrophobic disks at the lowest settings

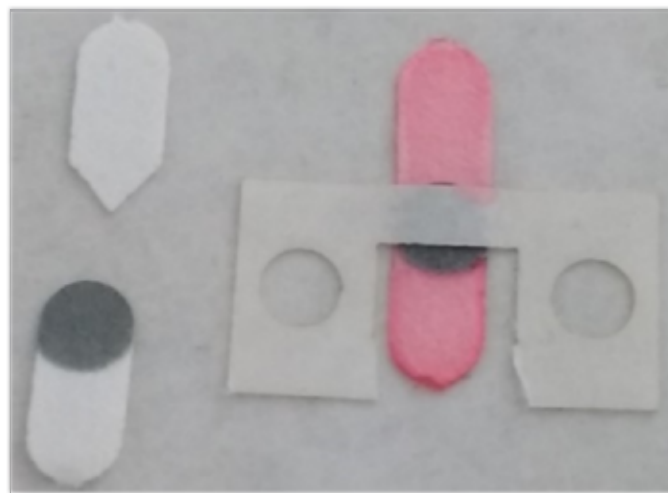


Figure 16. Wax Valve Prototype

This device showed better performance than the previous designs, but was still too prone to failure to be used in the final chip. The device went through numerous redesigns before it was eventually replaced with the much more reliable and simple to manufacture cantilever valve.

3.4.3 Cantilever Valve

In order to improve the reliability of the device, and remove some of the points of failure from the previous designs, a new valve design was implemented. The original idea was a bi-material cantilever valve conceived by Winfield "Wayne" Smith. Through observation of bi-material valve, a mono-material valve was also designed specifically for this project. The two devices were compared to determine which of them would be optimal for this particular application.

3.4.3.1 Bi-material Cantilever

The original bi-material valve concept was proposed by Winfield "Wayne" Smith. This design consisted of a strip of filter paper with tape applied to one side of it. When the strip is saturated, the paper extends slightly, while the tape remains the same length. This length differential causes the strip to bend slightly in the direction of the tape. This flex can be used to make connections to other fluidic circuits.

The chief disadvantages of this design are the difficulty of manufacture of the cantilever, and the need for multiple levels within the chip. Assembling these devices requires the placement of precision cut tape strips onto precision cut paper strips. Alignment is crucial for the valve to work as designed, so placing the tape strip consistently by hand without damaging the adhesive side of the tape or the paper strip itself is remarkably difficult. The need for multiple levels within the device arises as a result of bi-material valves normal operation. The bi-material

valve starts out as a straight strip until fluid is introduced, at which point it begins to curve in the direction of the tape backing. Therefore the device must have another level above or below the valve for it to contact and connect to as it flexes. Because of these shortcomings a more refined concept was tested.

3.4.3.2 Mono-material Cantilever

In testing the bi-material cantilever device, it was observed that bent strips of paper would return to their original position when saturated. Therefore, a new simplified design was proposed. With the elimination of the need for a tape backing, manufacture becomes easier. In addition to this, all the channels can be on the same plane without the need for multiple levels. This valve concept also allows for the fluid that triggers the valve to be isolated from the connections it makes. This opens up a host of options for new device designs options that extend well beyond the scope of this project. The only major disadvantage of this device is the fact that it requires clearance above the top of the chip for the cantilever to protrude. This will require a taller housing to contain it, meaning more material will be required and the device will be less compact. The advantages presented by this device were determined to far outweigh its disadvantages and therefore led to its adoption for use in the final device.

3.5 Valve Characterization

In order to use the new valve designs created for this study, their performance had to be characterized. Both devices were tested using a base that was designed in SolidWorks, and manufactured out of PLA using a 3D printer.



Figure 17. 3D printed valve test base

As seen in Fig. 17 the valve test holder was designed to support the edges of the test chip without interfering with the cantilever in the center. The small column in the center was included to allow the test holder to serve a secondary purpose that was never pursued, so it was snapped off with pliers prior to testing.

3.5.1 Bi-material Valve Testing

To evaluate the effectiveness of the bi-material valve, a batch of 15 cantilevers were manufactured and tested. Five of these tests were 15 by 4.5mm strips with with a 12.5 by 4.5 layer of tape backing, five were 20mm by 4.5mm with a 16mm by 4.5mm backing, and five were 20mm by 4.5mm with a 20mm by 4.5mm backing.

Each of the devices was printed and laser cut in the same manner as the other chip designs. The tests were affixed to the 3D printed base using double sided tape, and run with $20\mu\text{l}$ of water. The final position of the tip relative to its original position (final flex) was measured using digital calipers, and the results were recorded and summarized in section 4.

3.5.2 Mono-material Valve Testing

In order to ensure uniform flex, a jig was designed in SolidWorks and printed out of PLA using the Raise 3D printer. The jig was a 5 mm thick rectangle with a 5 mm tall triangle cut out of one side, as shown in Fig. 18.

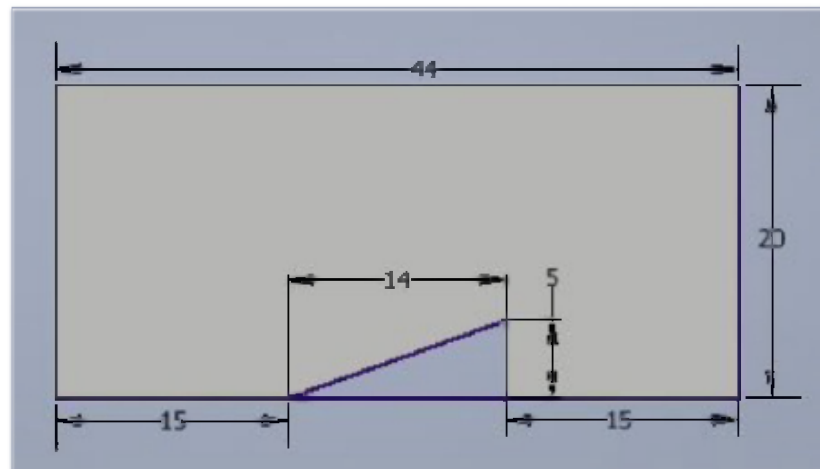


Figure 18. Cantilever Valve Bending Jig

The mono-material test strips were printed and laser cut in the same manner as the previous devices. some of the test strips are displayed in Fig.19.

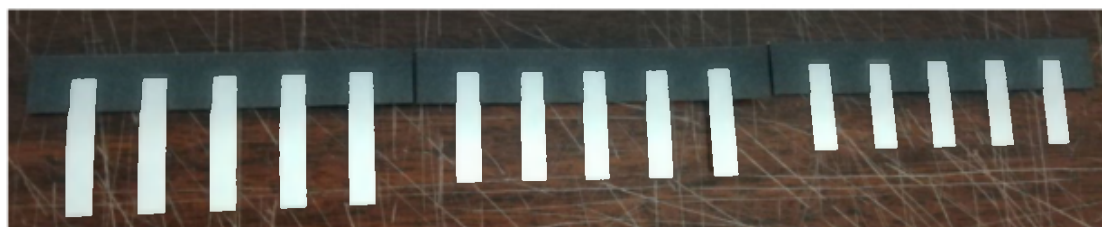


Figure 19. Mono-material Length Characterization Test

The mono material valve was characterized to determine the effect of length and width on it. The effect of the length was determined by running 5 10mm by 5.5 mm strips, 5 15 mm by 5.5 mm strips, and 5 20 mm by 5.5 mm strips. The mean final flex, as well as the time required for the fluid to reach the end of the strip was then recorded. Each of these tests was flexed 5 mm at the tip before testing using the jig, and $15\mu\text{l}$ of fluid was added via pipette to each in order to trigger them and ensure complete saturation.

The effect of the width was determined by running a series of 15 mm long cantilever strips with various widths under the same conditions. the widths selected were 3mm, 4mm, 5mm, 6mm, and 7mm. 3 tests were performed for each thickness, and the flex after wetting was measured using digital calipers.

The minimum fluid required to actuate the valve was determined by running a series of of identical tests with increasing fluid volume and recording how much each valve flexed. The 4.5 by 15 mm strips were flexed 5 mm up at the tip, and then wetted with with 1 to 8 μl of red dyed water. The distance from the papers original position was then measured for each using digital calipers.

In order to determine if the paper's behavior of returning to its original position when wetted was a result of gravity or the expansion and relaxation of the fibers within the paper, a test was performed where the device was placed at a 90 degree angle prior to being wetted. This way gravity would play no role in the movement of the chip and all flex observed could be attributed to the effects within the paper fibers. Each strip was bent back 5 mm, and $15\mu\text{l}$ of water was then applied to the supported portion of the strip. The final flex of the valve was then recorded using digital calipers.

3.6 SuperLoop Design

The fluidic circuit displayed in Fig. 13 was created using the same methods as the previous tests. The paper layers that make up the chip are displayed in Fig. 20.

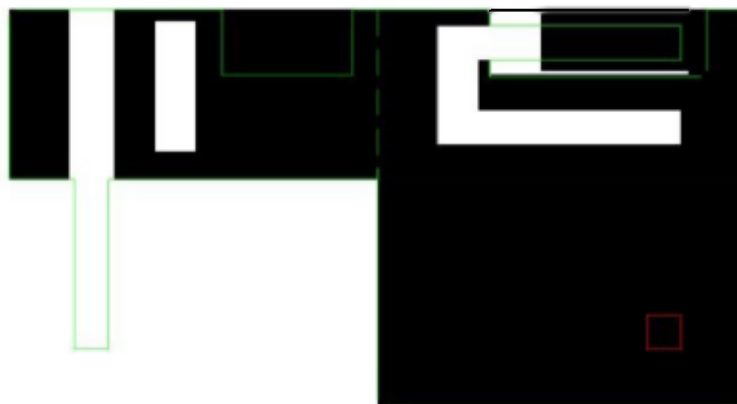


Figure 20. SuperLoop Chip Part

The SuperLoop device required the same active components as the unmodified pregnancy test, so the tests were disassembled into their component parts. The disassembled test is displayed in Fig. 21. Along the bottom of the figure, the test line, conjugate pad, and glass fiber inlet are aligned respectively. The conjugate pad and test line were integrated into the final SuperLoop device.



Figure 21. Disassembled Pregnancy Test

In Fig.21 the test line, conjugate pad, and glass fiber reservoir are laid out horizontally along the bottom from left to right. These components were then integrated into the final SuperLoop device.

3.7 Testing New Device

The new device was tested in two stages. The device was tested fluidically before moving on to testing with active components.

3.7.1 Fluidic Testing

During development, the device was tested fluidically to refine the concept without waisting expensive components and chemicals. For these tests, the wash and drive fluids were replaced with red and green dyed water, the test line was replaced with Whatman filter paper, and the conjugate pad was replaced with Millipore glass fiber.

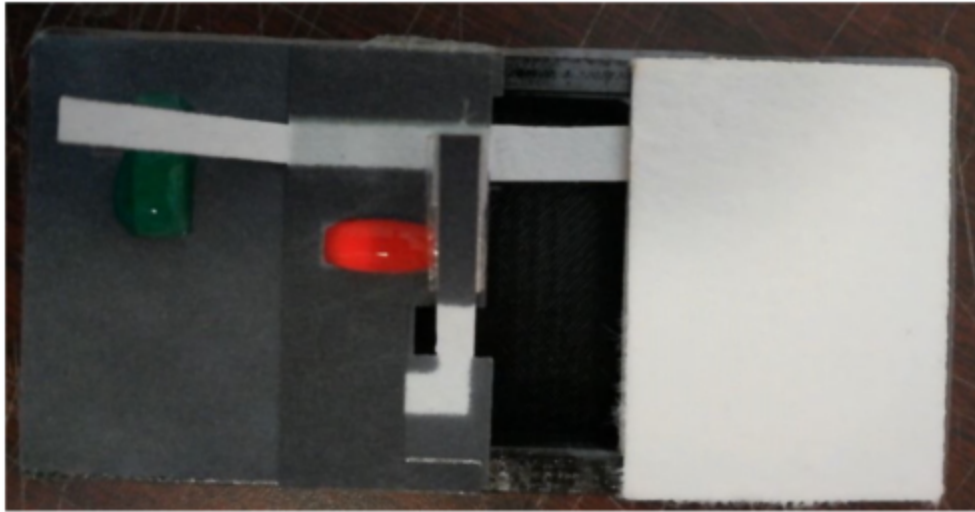


Figure 22. Fluidic SuperLoop Test

3.7.2 Hook Effect Mitigation Testing

In order to evaluate the effectiveness of the new devices, they must be compared to the original unmodified test. The tests must occur at concentrations both above and below the point where the hook effect occurs to ensure that the original function of the device is not impaired and the hook effect is mitigated. The signal will be evaluated numerically using the same methods that were used to isolate the hook effect in section 3.1. Each device was tested with $40\ \mu\text{l}$ of sample fluid to remain consistent with the previous tests.

3.7.3 Running and Scanning New Device

After assembly, each SuperLoop device was run using $100\ \mu\text{l}$ of buffer fluid on the wash pad, $80\ \mu\text{l}$ of buffer fluid on the drive pad, and $20\ \mu\text{l}$ of sample fluid on the sample line. The test was allowed to run until the fluid had drained from both the wash pad and drive fluid reservoir, and no fluid flow was visible on the test line. The test line was then extracted from the device so it could be scanned. The unmodified tests were run in much the same method as section 3.1. Each of these tests was run at 1x, 5X, 10X, 100X, and 1000X dilution a total of 3 times each

making for a total of 30 tests performed.

The scanning process for the new device had to be slightly modified to account for the fact that the test line was now removed from the housing prior to being scanned. In order to ensure parity of results with the modified test, the test line was also removed from the unmodified test prior to its scan. This allowed the test line to sit flat on the scan bed without any obstructions. The actual scan was carried out in the same method as section 3.1.

3.7.4 Processing results using ImageJ

Due to the irregularities in test line indication shape that are discussed in section 4, the test line was analyzed in two different ways. Both methods began with inverting the image much like in section 3.1. The key difference was the method used to select an area of the strip to apply the measure command in order to obtain a numerical value.

The first method used a 25 pixel by 25 pixel square. This square was positioned over the areas of the line that showed the greatest indication. The results were taken 5 times at different high indication areas, and the greatest value obtained was taken for the line.

The second method was similar method used in section 3.1. A large rectangle was drawn over the full area of the strip that showed a clear indication. In order to account for user error, the greatest value obtained after five separate scans of the same line was used in the following calculations.

The mean of the values obtained from the 3 tests for each concentration was then calculated for both methods, and the results were used to create graphs comparing the performance of the modified and unmodified tests.

CHAPTER 4

Findings

This chapter collects the results of all experiments performed over the course of this research.

4.1 Isolation of the Hook Effect

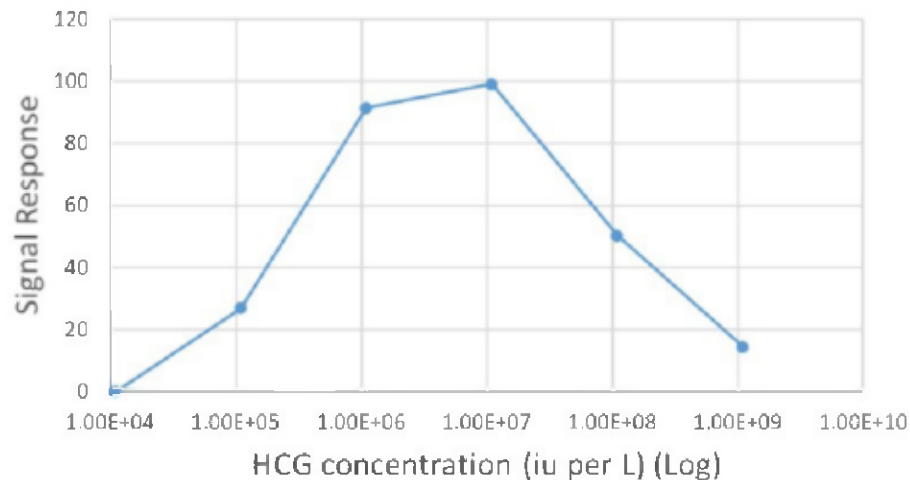


Figure 23. Signal Response Over hCG Concentration in Common Pregnancy Tests

Here the Hook Effect is viable across the blue signal line, as the increased concentration of hormone results in a decreased signal response. The Hook Effect occurs between 1.00E+6 to 1.00E+9 IU/L in these devices, so that is the range that the Hook Effect mitigation device will be tested across.

4.2 Characterization of the Cantilever Valve

Separate tests were performed on the bi-material and mono-material cantilever valves in order to determine which would be selected for use in the final device.

4.2.1 Bi-Material Valve Characterization

The results of the bi-material valve test are as follows: The valve showed

Table 1. Bi-material Cantilever Performance

Paper Strip Length(mm)	Tape Backing Length(mm)	Mean Final Flex (mm)
15	12.5	≈ 2
20	16	≈ 3
20	20	≈ 3.5

consistent performance in all 3 scenarios, with all 5 being approximately equal to the integer value displayed. The values are marked as approximate due to the difficulties of measuring anything smaller than quarter millimeters by hand. The valves showed usable performance, but the requirement of designing and building chips with multiple layers separated by 3 mm at most would introduce unnecessary complexity to the device.

4.2.2 Mono-Material Valve Characterization

The results of the mono-material valve tests are described in detail in the following sections.

4.2.2.1 Effect of Length on Mono-Material Performance

Table 2. Mono-material Cantilever Performance With Various Lengths

Length (mm)	Mean opening time(s)	Mean Final Flex (mm)
10	4.8	>1
15	10.6	<1
20	21.2	<1

The mean final flex is once again marked as approximate due to the difficulties of measuring anything smaller than quarter millimeters by hand. The results varied very little with length, as most of the flex occurs within the area of the strip where the supported section meets the unsupported section. Therefore the length makes very little difference to flex.

The time on the other hand, is greatly affected by the strip length. This is mostly due to the measurement method that was described in section 3. The valve

was considered "open" when the fluid reached the end of the strip. In retrospect this was not the best way to measure the opening time, as the strip begins to flex almost immediately. In all three cases, the strip flexed most of the way within three seconds; the time after that was just the fluid continuing to flow down the strip until it reached the end. In the actual valve, the channel will touch the contact point on the other side of the valve and begin absorbing fluid from it before the triggering fluid reaches the end, so these data were not actually helpful. Nevertheless, this test did confirm the effectiveness of the valve, as a mean final flex of <1 mm is sufficient to make contact with the fluid waiting on the other side of the valve.

4.2.2.2 Effect of Width on Mono-Material Performance

The test performed affirmed the theoretical prediction that width would have no noticeable effect on the performance of the valve.

Table 3. Mono-material Cantilever Performance With Various Widths

Width (mm)	Mean Final Flex (mm)
3	≈1
4	≈1
5	≈1
6	≈1
7	≈1

Due to this finding, the width of strips within the final device could be chosen based on the required geometry alone, without need for concern for valve performance.

4.2.2.3 Minimum Fluid Required for Valve Actuation

Fig.24 shows the outcome of the minimum fluid actuation test, the results of which are summarized in table 4.

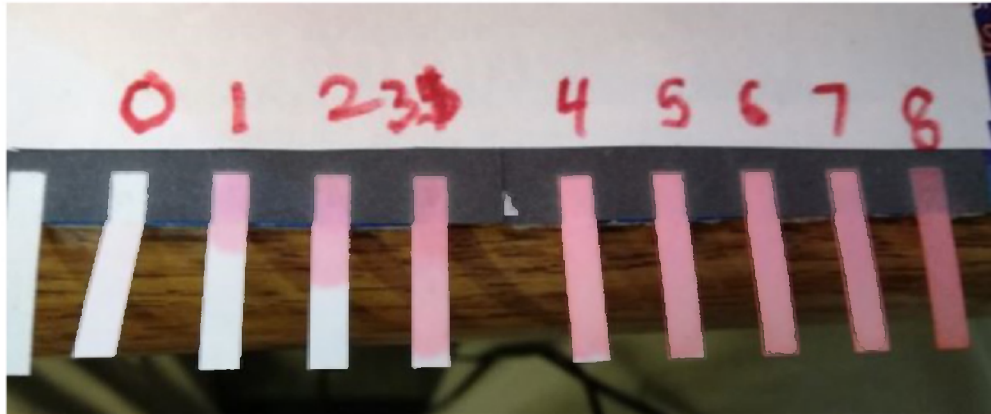


Figure 24. Results of Mono-Material Minimum Fluid Test

Table 4. Mono-material Cantilever Performance With Various Fluid Volumes

Fluid Volume (μl)	Mean Final Flex (mm)
1	≈ 2
2	> 1
3	< 1
4	< 1
5	< 1
6	< 1
7	< 1
8	< 1

Any volume of fluid greater than $3 \mu\text{l}$ proved adequate to actuate the valve. This was expected, as the bend was applied to the area of the strip where the unsupported part meets the supported part, with the effort being made to ensure that the rest of the strip remains straight. Therefore only the beginning portion of the cantilever has to be saturated to actuate the valve fully.

4.3 SuperLoop Hook Effect Mitigation Results

The results of the SuperLoop device scan analysis are displayed in the following graphs.

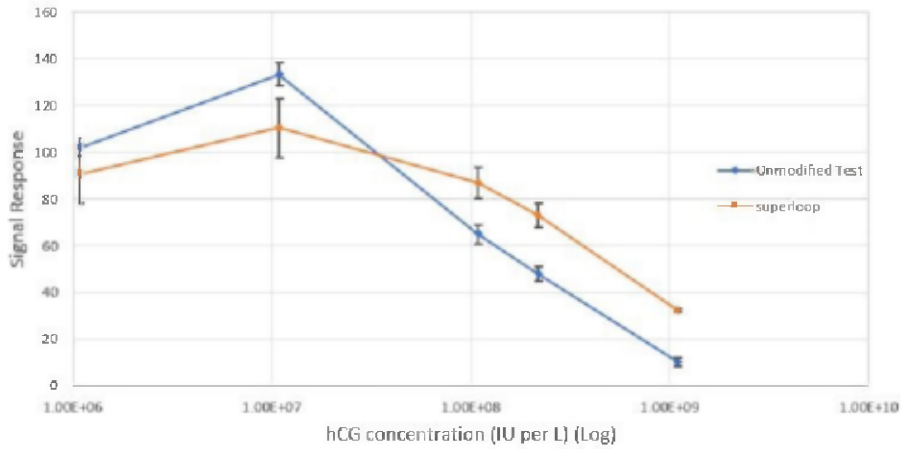


Figure 25. 25 by 25 Scan of SuperLoop vs Unmodified Device

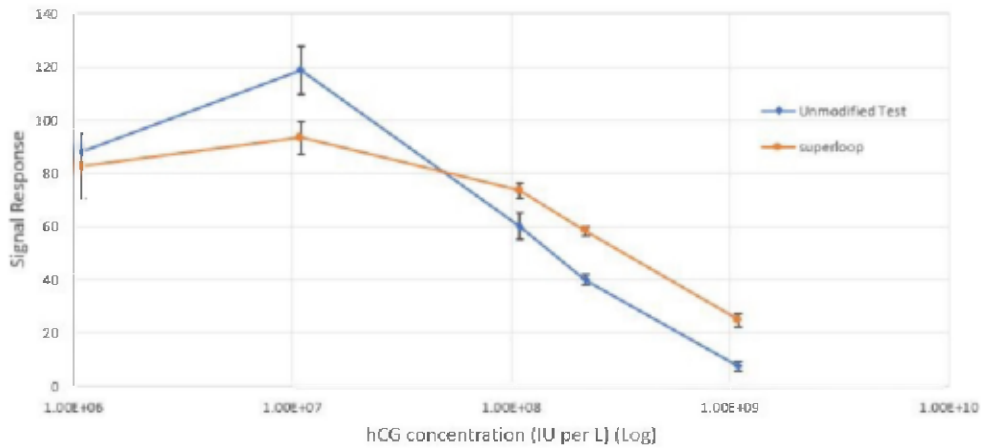


Figure 26. Full Area Scan of superLoop vs Unmodified Device

Both graphs show similar performance, so the choice of analysis method does not affect the conclusions that can be formed from the data. In order to better represent the Hook Effect reduction of the SuperLoop device, both sets of signal data were normalized.

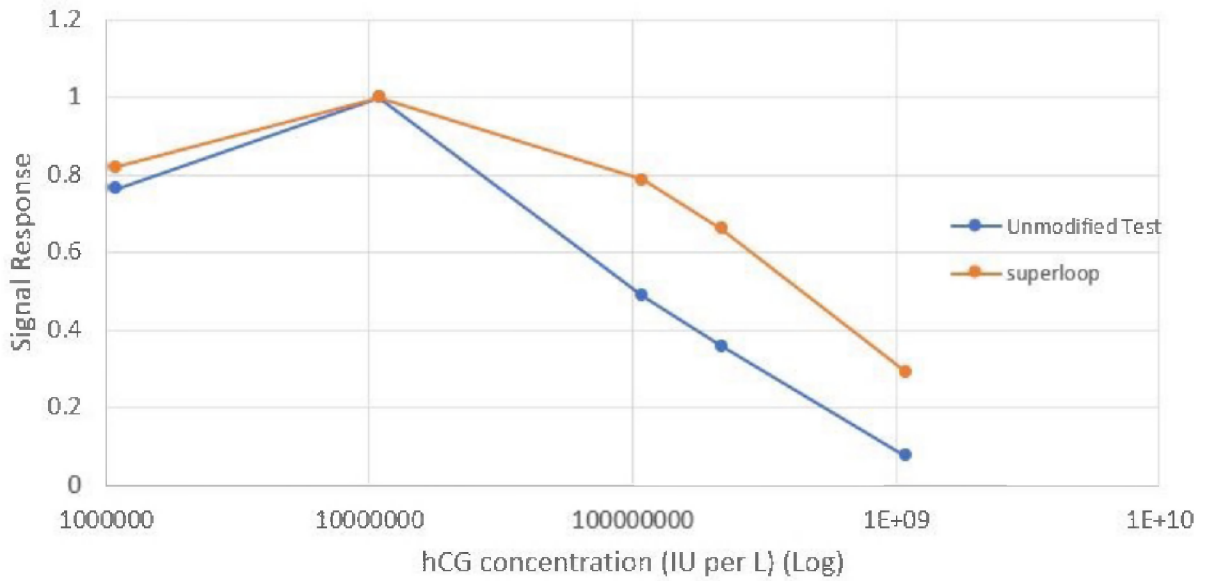


Figure 27. 25 by 25 Scan of SuperLoop vs Unmodified Device Normalized

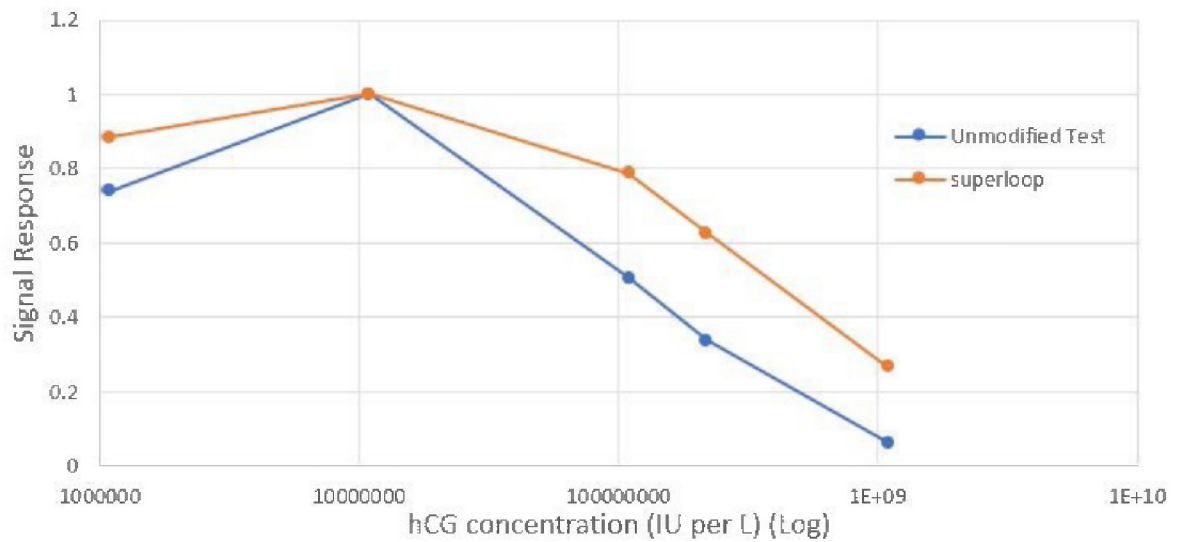


Figure 28. Full Area Scan of superLoop vs Unmodified Device Normalized

While the device was not able to completely eliminate the hook effect, it did do a great deal to mitigate it. The following table gives performance data:

Table 5. Performance of SuperLoop vs ordinary test at hook effect concentrations

Test	Minimum	Maximum	Difference
25x25 Unmod	10.09	103.22	123.13
25x25 SuperLoop	32.21	110.32	78.12
Full Unmod	7.37	118.76	111.39
Full SuperLoop	24.81	93.27	68.46

The device helps to smooth out the graph of signal response. The SuperLoop provides a 36.6% reduction in spread by the 25X25 analysis method, and a 38.5% reduction in spread by the full block analysis method. This serves as an excellent proof of concept And could potentially be developed into a fully viable commercial product.

CHAPTER 5

Conclusion

The completion of this study has yielded a device that successfully mitigates the Hook Effect. While the effect was not completely eliminated, as was the original goal of the research, the results obtained by the final SuperLoop device serve as an adequate proof of concept. The cantilever valve that was developed over the course of the research is also a triumph in and of itself. Both of these achievements will serve to further the field of micro fluidics. In addition to this, the research served to further develop the engineering skills of the student.

5.1 Future Work

Over the course of this research a great deal of progress was made not just in the field of Hook Effect Mitigation, but also in microfluidic device design as a whole. This new device requires further refinement to become a viable commercial product, but nonetheless shows great promise now as a potential addition to future microfluidic tests of all types. The cantilever microfluidic valve has untold potential applications that future research may unlock.

5.1.1 Hook Effect Mitigation Device Refinements

While this new device shows a great deal of promise, several improvements would have to be made in order to transform it into a viable commercial product.

5.1.1.1 Assembly Methods and Materials

One of the greatest difficulties encountered in the production of these devices was the problem of hand assembly. The slightest variation in the position of components within a chip could lead to leaks or other performance issues. A great deal of the design process was spent finding ways around these limitations through

the use of jigs, folding components, and a great deal of practice laying parts down consistently. Many tests had to be discarded before they were even run due to manufacturing irregularities. Methods to eliminate these problems would allow more devices to be tested faster, and would thus serve to further enhance reliability.

5.1.1.2 Housing Refinement

Several improvements to the housing could make the SuperLoop device more robust and effective. An enhanced top layer that holds the bent cantilevers in place would offer several benefits. In addition to protecting the device from debris and structural damage, it would ensure that the cantilevers remained perfectly positioned to flex upon activation. It could even be designed so that the user has to "snap" it into an active position before the sample can be added. Upon snapping it into place, the sample area would be exposed, and the cantilevers would be released. This way the device would be resistant to user error as well as the hook effect. The top could also hold the fluid reservoirs in sealed chambers that open when the device is activated. This way when the user snaps the device into action, the fluid flows into the wash and drive pads where it is retained until the cantilever valves are activated by the addition of the sample fluid.

5.1.1.3 Miniaturization

This area of future progress goes hand in hand with the previous two. The main reason for the size of the current device is the fact that it was designed for hand assembly. Some type of automated manufacture or greatly simplified, tool assisted assembly method would allow much of the unnecessary material to be removed from the device. A robust housing would help to ensure the safety of the smaller internal components, making miniaturization a more definite possibility. Miniaturization would reduce the amount of materials required to manufacture

this device, making it more commercially viable.

5.1.2 Applying SuperLoop device to other Sandwich ELISA Tests

While pregnancy tests were selected as the subject of this research, future iterations of the SuperLoop could easily be adapted to other Sandwich ELISA style tests. As previously discussed, the Hook Effect has been observed in other types of tests as well, so any of them would make a good target for the next iteration of this device.

5.1.3 Future Applications of Cantilever Valve

Future projects performed in the microfluidics laboratory, as well as those conceived in other labs as a result of the publication of this thesis, will be able to take advantage of the mono-material cantilever valve to make reliable automated fluidic connections within their devices. Combining this with delay channels, fluid reservoirs, and some clever engineering will allow for any type of chemical reaction to be controlled and automated within a paper chip. The observable, physical nature of these valves will also make them an attractive choice for engineers looking for a fluidic valve to use in their devices. They are easy to manufacture, and can be observed functioning, allowing for easier data collection during device tests. Being able to watch the device work, rather than merely observe the final results, allows problems in the device to be isolated and fixed faster. For all these reasons, it is believed that mono-material cantilever valves will begin appearing in other devices in the near future.

5.1.4 Continuation of Abandoned Valve concepts

Over the course of this research, many device configurations were created, tested, and discarded in favor of a new idea. While the cantilever valve did prove the most robust and easy to manufacture, any of the previous valve concepts could

potentially be refined to the same level of performance. The greatest limitation in this study was the unpredictability introduced by hand assembly, so a revised manufacture method that mitigates this effect could potentially enhance the reliability of these devices. The core concepts behind each of the old valve designs are solid, it would merely be a matter of finding better ways to implement them.

LIST OF REFERENCES

- [1] EDM Millipore. “Rapid lateral flow test strips: Considerations for product development.” Two separate URLs included, one for a sideshow the other for its companion document. [Online]. Available: https://www.emdmillipore.com/INTERSHOP/static/WFS/Merck-Site/-/Merck/en_US/Freestyle/DIV-Divisional/Events/pdfs/lateral-flow-presentations/design-considerations-for-lateral-flow-test-strips.pdf, https://www.emdmillipore.com/Web-US-Site/en_CA/-/USD/ShowDocument-Pronet?id=201306.12550
- [2] Y. Yadav, U. Fatima, S. Dogra, and A. Kaushik, “Beware of hook effect giving false negative pregnancy test on point-of-care kits,” *Journal of Postgraduate Medicine*, vol. 59, pp. 153–154, 2013.
- [3] R. T. Griffey, C. J. Trent, R. A. Bavolek, J. B. Keeperman, C. Sampson, and R. F. Polrier, “Hook-like effect causes false-negative point-of-care urine pregnancy testing in emergency patients,” *Journal of Emergency Medicine*, vol. 44, pp. 155–160, 2013.
- [4] J. Chen, K.-H. Chen, L.-M. Wang, W.-W. Zhang, L. Feng, H.-Z. Dai, and Y.-N. He, “High-dose hook effect in urinary dcr2 assay in patients with chronic kidney disease,” *Clinical Biochemistry*, vol. 58, pp. 32–36, 2018.
- [5] N. Walji and B. D. MacDonald, “Inuence of geometry and surrounding conditions on fluid flow in paper-based devices,” *Micromachines*, 2016.
- [6] W. Fllscher, “Development of a platform for lateral flow test devices with the capability of using multiple fluids,” 2013.
- [7] R. Sidana, H. C. Mangala, S. B. Murugesh, and t. . K. Ravindra.
- [8] Markets and Markets. “Point-of-care/rapid diagnostics market by testing (glucose, lipids, hba1c, hcv, hiv, influenza, urinalysis, hematology, cancer, pregnancy, pt/inr), platform (lateral flow, immunoassay), mode (prescription, otc), end-user - global forecast to 2022.” Feb. 2018. [Online]. Available: <https://www.marketsandmarkets.com/Market-Reports/point-of-care-diagnostic-market-106829185.html>
- [9] A. D. Winder, A. S. Mora, E. Berry, and J. R. Lurain, “The hook effect causing a negative pregnancy test in a patient with an advanced molar pregnancy,” *Gynecologic Oncology Reports*, vol. 21, pp. 34–36, 2017.
- [10] M. Muller, “Enzymatic and enzyme inhibitory activity on a paper based lateral flow device,” 2015.

- [11] B. Li, L. Yu, J. Qi, L. Fu, P. Zhang, and L. Chen, “Controlling capillary-driven fluid transport in paper-based microfluidic devices using a movable valve,” *Analytical Chemistry*, vol. 89, no. 11, pp. 5707–5712, 2017.
- [12] A. C. Mitropoulos, “Capillarity,” *Journal of Engineering Science and Technology Review*, vol. 2, pp. 28–32, 2009.

BIBLIOGRAPHY

Epilog laser mini 18/24 and helix laser manual, Dec 2016.

Chen, J., Chen, K.-H., Wang, L.-M., Zhang, W.-W., Feng, L., Dai, H.-Z., and He, Y.-N., “High-dose hook effect in urinary dcr2 assay in patients with chronic kidney disease,” *Clinical Biochemistry*, vol. 58, pp. 32–36, 2018.

EDM Millipore. “Rapid lateral flow test strips: Considerations for product development.” Two separate URLs included, one for a sideshow the other for its companion document. [Online]. Available: https://www.emdmillipore.com/INTERSHOP/static/WFS/Merck-Site/-/Merck/en_US/Freestyle/DIV-Divisional/Events/pdfs/lateral-flow-presentations/design-considerations-for-lateral-flow-test-strips.pdf, https://www.emdmillipore.com/Web-US-Site/en_CA/-/USD/ShowDocument-Pronet?id=201306.12550

Fllscher, W., “Development of a platform for lateral flow test devices with the capability of using multiple fluids,” 2013.

Griffey, R. T., Trent, C. J., Bavolek, R. A., Keeperman, J. B., Sampson, C., and Polrier, R. F., “Hook-like effect causes false-negative point-of-care urine pregnancy testing in emergency patients,” *Journal of Emergency Medicine*, vol. 44, pp. 155–160, 2013.

Li, B., Yu, L., Qi, J., Fu, L., Zhang, P., and Chen, L., “Controlling capillary-driven fluid transport in paper-based microfluidic devices using a movable valve,” *Analytical Chemistry*, vol. 89, no. 11, pp. 5707–5712, 2017.

Markets and Markets. “Point-of-care/rapid diagnostics market by testing (glucose, lipids, hba1c, hcv, hiv, influenza, urinalysis, hematology, cancer, pregnancy, pt/inr), platform (lateral flow, immunoassay), mode (prescription, otc), end-user - global forecast to 2022.” Feb. 2018. [Online]. Available: <https://www.marketsandmarkets.com/Market-Reports/point-of-care-diagnostic-market-106829185.html>

Mitropoulos, A. C., “Capillarity,” *Journal of Engineering Science and Technology Review*, vol. 2, pp. 28–32, 2009.

Muller, M., “Enzymatic and enzyme inhibitory activity on a paper based lateral flow device,” 2015.

Nerenz, R. D., Butch, A. W., Woldemariam, G. A., Yarbrough, M. L., Grenache, D. G., and Gronowski, A. M., “Estimating the hcg β cf in urine during pregnancy,” *Clinical Biochemistry*, vol. 49, pp. 282–286, 2016.

Sidana, R., Mangala, H. C., Muruges, S. B., and K. Ravindra, t. .

Walji, N. and MacDonald, B. D., “Inuence of geometry and surrounding conditions on fluid flow in paper-based devices,” *Micromachines*, 2016.

Winder, A. D., Mora, A. S., Berry, E., and Lurain, J. R., “The hook effect causing a negative pregnancy test in a patient with an advanced molar pregnancy,” *Gynecologic Oncology Reports*, vol. 21, pp. 34–36, 2017.

Yadav, Y., Fatima, U., Dogra, S., and Kaushik, A., “Beware of hook effect giving false negative pregnancy test on point-of-care kits,” *Journal of Postgraduate Medicine*, vol. 59, pp. 153–154, 2013.